Journal of Control, Automation and Electrical Systems (2020) 31:548–556
https://doi.org/10.1007/s40313-020-00563-2

Use of Flatness-Based Control as Feedforward Compensator for an Aeronautical Pneumatic System

Dayvis D. Silva[1] · **Takashi Yoneyama**[2]

Received: 18 September 2019 / Revised: 4 December 2019 / Accepted: 7 January 2020 / Published online: 29 January 2020

Abstract
The idea in this work is to explore the use of flatness technique in the context of application to the problem of temperature regulation of an aeronautical system. More specifically, the integrator windup phenomenon (typical of PID control) is evaluated and the use of flatness-based control is proposed as an alternative solution. Comparison between the proposed technique with a traditional anti-windup technique available in the literature is provided based on simulation results using a model with the structure validated with real experimental data and with realistic parameter values.

Keywords Aeronautical pneumatic systems · Nonlinear control · Flatness · Feedforward · Windup

1 Introduction

As presented in Silva and Yoneyama (2018), the purpose of the aeronautical pneumatic system is to supply compressed air bled from the aircraft engines to the various consumer systems such as air conditioning, cabin pressurization, anti-ice, fuel tank inertization, cross-engine starting and others. It is composed by valves, sensors, controller and ducts for air distribution at low and high pressures. The design of a control law for this system (pressure and temperature control) tends to present a considerable challenge due to the inherent nonlinearities (air flow Andersen (2001) and heat transfer Incropera and Dewitt (1998) equations) and large range of operational conditions. In aeronautical applications, it is common the use of PID controllers (proportional–integral–derivative), which is well studied for application to linear systems, although it may also be found in nonlinear control loops. Linear control theory provides a variety of powerful tools for analysis and design of linear systems, as presented in Ogata (2003). On the other hand, for nonlinear system, some approaches may provide very good results for some specific class of systems but not for others. In this context, the work presented in Silva and Yoneyama (2018) evaluates the application of some nonlinear control techniques to the temperature control of an aeronautical pneumatic system. There are some other examples of nonlinear control techniques for this kind of system, such as those based on LPV models (linear parameter varying) Turcio et al. (2013) and feedback linearization Turcio et al. (2014) and Silva et al. (2014). However, the aeronautical field tends to be conservative and attached to the well-conceived methods. Based on that, in this work, it is explored the benefits of flatness-based control Fliess et al. (1995, 1999) without given up from the PID, in which a combined architecture using both techniques is proposed.

The concept of flatness technique has been used in Martin (1994, 1996) for trajectory control of aircrafts and in Koo and Sastry (1999), Koo et al. (2001) for the case of helicopters. Here, the purpose is to extend the application of flatness-based control to the field of aeronautical engineering for tasks other than the tracking of flight trajectory. In Rigatos et al. (2016), for example, the flatness concept is proposed for the control of turbocharged diesel engines.

This work is organized as follows: Sect. 2 concerns the motivation for studying the use of flatness-based control combined with a PID for aeronautical pneumatic system; an overview of the system under study is presented in Sect. 3; Sect. 4 introduces the mathematical model; Sect. 5 presents the control laws development; Sect. 6 is dedicated to simula-

✉ Dayvis D. Silva
dayvis.silva@embraer.com.br

Takashi Yoneyama
takashi@ita.br

[1] Control Systems Engineer at EMBRAER, São José dos Campos, SP, Brazil

[2] Department of Systems and Control, ITA- Instituto Tecnológico de Aeronáutica, São José dos Campos, SP, Brazil

tion results and discussion; finally, Sect. 7 presents the main conclusions.

2 Motivation

The motivation for this study is supported by the challenges in the design and control of pneumatic systems when integrated in the aircraft. The main challenges may be listed in a concise form as provided below:

- nonlinearities: friction, backlash, hysteresis, dead zones, saturation, airflow, heat transfer, etc;
- variety of operational/flight conditions and altitude: take-off, climb, cruise, descent, holding, approach, landing and taxi;
- different aircraft engine power rates, auto-throttle;
- different demand configurations: ECS on/off (air conditioning and pressurization systems), anti-ice on/off, dual/single bleed (dual or single engine availability as pneumatic source), etc;
- differences in the performance of the components associated with dispersion of the true parameters values with respect to the nominal values due to manufacturing variations, wear and aging.

In addition, when controlling a system over a wide range of operation, one should consider the nonlinear effect of actuator saturation. For controllers with integral action, the feedback loop is broken when the actuator saturates and the system output may be drift to undesirable values. The consequences are that it may take a long time for the system to reach equilibrium after an upset. Such phenomenon was first noticed in conventional PID control and is therefore called integrator windup.

Thus, in this work, an alternative strategy for dealing with the windup phenomenon is proposed, but instead of "avoiding" the windup itself, the proposal enables the system to recover from the windup condition in a time sufficiently fast so that the consequences of the windup are minimized. In such proposal, a flatness-based control strategy is combined with a PID, acting like a feedforward compensator for the last one.

For comparison purpose, an anti-windup technique with a conventional PID is also evaluated. The anti-windup technique implemented is based on one of the possible solutions described in Astrom and Rundqwist (1989), defined as back-calculation (ad hoc method). Several other methods are available in the literature, as those presented in Hadade Neto (2005), in which 12 different linear and nonlinear anti-windup techniques are assessed. In addition, results for flatness technique architecture, as proposed in Silva and Yoneyama (2018), and a simple PID architecture without any anti-windup technique are also presented.

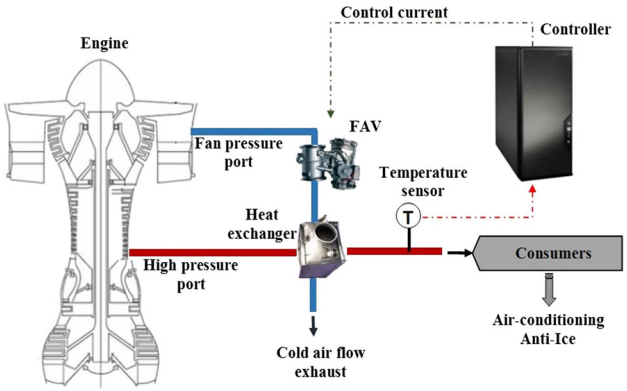

Fig. 1 Schematic representation of the aeronautical pneumatic system under study

3 Problem Presentation

The plant to be controlled is the same as studied in Silva and Yoneyama (2018), in which the system has a hot and a cold side. The cold side is composed by a pneumatic regulator valve (FAV: fan air valve), a heat exchanger (pre-cooler), a temperature sensor, a controller and the ducts that allow the flow of air from the cold source to the atmosphere. A schematic representation of the system under study is presented in Fig. 1.

As shown in Fig. 1, the hot air from high pressure port of the engine compressor is cooled in a compact cross-flow heat exchanger. The cold air from the fan pressure port of the engine, used for cooling down the hot air flow, is discharged in the atmosphere after flowing through the heat exchanger. The temperature of the hot air flow downstream the heat exchanger is measured by a temperature sensor. The controller receives the information of the measured temperature and generates the control current for the FAV, which modulates the cold air flow in order to control the temperature in accordance with the temperature reference.

The FAV is one of the most important components in the temperature loop. A typical architecture for this type of valve is shown in Fig. 2.

4 Mathematical Model

The system under study can be represented by five nonlinear ordinary differential equations, as given from 1 to 5.

$$\dot{P}_{\text{cin}} = f_0(P_{\text{cin}}, P_{\text{cout}}, T_{\text{cin}})P_{\text{cin}} + f_2(P_{\text{infav}}, P_{\text{cin}}, T_{\text{cin}}, x_v)x_v, \quad (1)$$

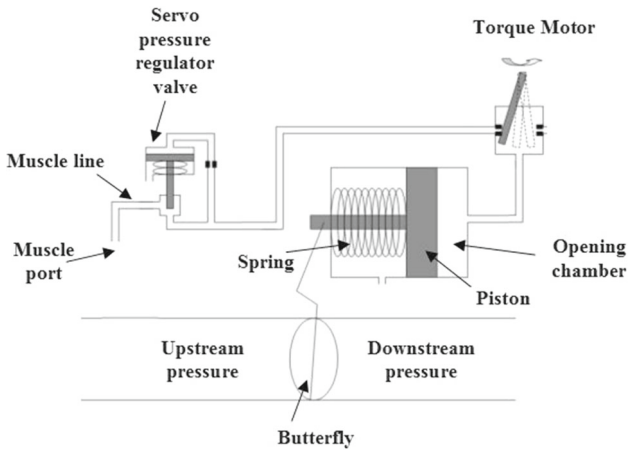

Fig. 2 Typical architecture of a FAV

$$\dot{P}_{\text{cfav}} = f_1(P_{\text{prv}}, P_{\text{cfav}}, T_{\text{amb}})P_{\text{cfav}} + f_3(P_{\text{prv}}, P_{\text{cfav}}, P_{\text{amb}}, T_{\text{amb}}, x_v)i, \tag{2}$$

$$\ddot{x}_v = \frac{A_1}{m}P_{\text{cfav}} - \frac{b}{m}\dot{x}_v - \frac{K_m}{m}x_v - \frac{A_2}{m}P_{\text{amb}} - \frac{P_L}{m}, \tag{3}$$

$$\dot{T}_{\text{Hout2}} = f_4(T_{\text{Hin}}, T_{\text{cin}}, \dot{m}_H, \dot{m}_c) \times f_5(P_{\text{cin}}, P_{\text{cout}}, T_{\text{cin}})P_{\text{cin}} - \frac{1}{\tau_{\text{pc}}}T_{\text{Hout2}}, \tag{4}$$

$$\dot{T}_{\text{Hout3}} = \frac{1}{\tau_s}T_{\text{Hout2}} - \frac{1}{\tau_s}T_{\text{Hout3}}. \tag{5}$$

They are composed by six state components, seven disturbance variables and one control input.

The state components are:

- P_{cin}: Heat exchanger cold side inlet pressure;
- P_{cfav}: FAV opening chamber pressure;
- x_v: FAV piston position;
- $\dot{x}_v$: FAV piston velocity;
- T_{Hout2}: Heat exchanger hot side outlet temperature;
- T_{Hout3}: Heat exchanger hot side regulated temperature measured by the temperature sensor.

The disturbance components are:

- P_{infav}: FAV inlet pressure;
- P_{cout}: Heat exchanger cold side outlet pressure;
- P_{amb}: Environment (ambient) pressure;
- T_{Hin}: Heat exchanger hot side inlet temperature;
- T_{cin}: Heat exchanger cold side inlet temperature;
- T_{amb}: Environment (ambient) temperature;
- $\dot{m}_H$: Hot air mass flow rate,

and the control input is:

- i: FAV torque motor control current.

The parameters A_1, A_2, b, K_m, m and P_L, in Eq. 3, represent the piston area of the opening chamber, the piston area of the closing chamber (which is pressurized by the environment pressure only), the viscous friction coefficient of the mechanical parts of the valve, the spring stiffness, the mass of the piston actuator and the FAV's spring preload, respectively. The parameter P_{prv}, in Eq. 2, is the pressure inlet torque motor regulated by the servo pressure regulator valve. The parameters τ_{pc} and $\dot{m}_c$, in Eq. 4, and τ_s, in Eq. 5, are the time constant (related to the thermal inertia) of the heat exchanger, the cold air mass flow rate and the temperature sensor time constant (thermal inertia), respectively.

The nonlinearities of the system are contained in the terms f_0, f_1, f_2, f_3, f_4 and f_5, which are given by Eqs. 6, 7, 8, 9, 10 and 11, respectively:

$$f_0 = -\frac{1}{V_{\text{pcin}}}(N_{\text{pcin}}K_{\text{pcin}}b_{\text{pc}}R\sqrt{T_{\text{cin}}}), \tag{6}$$

$$f_1 = \frac{1}{V_L + A_1x_v}(N'_{\text{prv}}K_{prv}P_{\text{prv}}b_{tm\_in}R\sqrt{T_{\text{amb}}}) - \frac{1}{V_L + A_1x_v}(N_{\text{pcfav}}K_{\text{pcfav}}b_{\text{tm\_out}}R\sqrt{T_{\text{amb}}} + A_1\dot{x}_v), \tag{7}$$

$$f_2 = \frac{1}{V_{\text{pcin}}}(N_{\text{infav}}K_{\text{infav}}P_{\text{infav}}b_{\text{but}}x_vR\sqrt{T_{\text{cin}}}), \tag{8}$$

$$f_3 = \frac{R\sqrt{T_{\text{amb}}}}{V_L + A_1x_v}(N_{\text{prv}}K_{\text{prv}}P_{\text{prv}}a_{\text{tm\_in}} - N_{\text{pcfav}}K_{pcfav}P_{\text{cfav}}a_{\text{tm\_out}}), \tag{9}$$

$$f_4 = \left[\frac{T_{\text{Hin}}}{\dot{m}_c} - \frac{\epsilon}{\dot{m}_H}(T_{\text{Hin}} - T_{\text{cin}})\right], \tag{10}$$

$$f_5 = \left(N_{\text{pcin}}K_{\text{pcin}}b_{\text{pc}}\frac{\sqrt{T_{\text{cin}}}}{T_{\text{cin}}}\right). \tag{11}$$

The parameters b_{pc}, $b_{\text{tm\_in}}$, $b_{\text{tm\_out}}$, b_{but}, $a_{\text{tm\_in}}$ and $a_{\text{tm\_out}}$ are, respectively: the equivalent orifice of the heat exchanger's cold side, of the torque motor from the muscle line to the inlet opening chamber (fixed value), of the torque motor from the opening chamber to the environment (fixed value), of valve's butterfly as a function of position, of the torque motor from muscle line to the inlet opening chamber as a function of control current and of the torque motor from the opening chamber to the environment as a function of control current. The parameters R, ϵ, V_{pcin} and V_L are, respectively: the gas constant of the air Van Wylen et al. (1998), the heat exchanger's thermal effectiveness, the heat exchanger's cold side inlet volume and the torque motor's line volume (from outlet servo pressure regulator to FAV opening chamber). The parameters K_{pcin}, K_{prv}, K_{pcfav}, K_{infav}, N_{pcin}, N_{prv}, N_{pcfav}, N_{infav} and N'_{prv} represent the compressible flow coefficients Andersen (2001), and they are given in Eqs. 12, 13, 14, 15, 16 and 17.

$$K_{\text{pcin}} = K_{\text{prv}} = K_{\text{pcfav}} = K_{\text{infav}} = \left[\frac{\gamma}{R}\left(\frac{2}{\gamma+1}\right)^{\frac{\gamma+1}{\gamma-1}}\right]^{1/2}, \tag{12}$$

$$N_{\text{pcin}} = \left[\frac{\left(\frac{P_{\text{cout}}}{P_{\text{cin}}}\right)^{2/\gamma} - \left(\frac{P_{\text{cout}}}{P_{\text{cin}}}\right)^{\frac{\gamma+1}{\gamma}}}{\left(\frac{\gamma-1}{2}\right)\left(\frac{2}{\gamma+1}\right)^{\frac{\gamma+1}{\gamma-1}}}\right]^{1/2}, \tag{13}$$

$$N_{\text{prv}} = \left[\frac{\left(\frac{P_{\text{cfav}}}{P_{\text{prv}}}\right)^{2/\gamma} - \left(\frac{P_{\text{cfav}}}{P_{\text{prv}}}\right)^{\frac{\gamma+1}{\gamma}}}{\left(\frac{\gamma-1}{2}\right)\left(\frac{2}{\gamma+1}\right)^{\frac{\gamma+1}{\gamma-1}}}\right]^{1/2}, \tag{14}$$

$$N_{\text{pcfav}} = \left[\frac{\left(\frac{P_{\text{amb}}}{P_{\text{cfav}}}\right)^{2/\gamma} - \left(\frac{P_{\text{amb}}}{P_{\text{cfav}}}\right)^{\frac{\gamma+1}{\gamma}}}{\left(\frac{\gamma-1}{2}\right)\left(\frac{2}{\gamma+1}\right)^{\frac{\gamma+1}{\gamma-1}}}\right]^{1/2}, \tag{15}$$

$$N_{\text{infav}} = \left[\frac{\left(\frac{P_{\text{cin}}}{P_{\text{infav}}}\right)^{2/\gamma} - \left(\frac{P_{\text{cin}}}{P_{\text{infav}}}\right)^{\frac{\gamma+1}{\gamma}}}{\left(\frac{\gamma-1}{2}\right)\left(\frac{2}{\gamma+1}\right)^{\frac{\gamma+1}{\gamma-1}}}\right]^{1/2}, \tag{16}$$

$$N'_{\text{prv}} = \left[\frac{\frac{(P_{\text{cfav}})^{2(1-\gamma)/\gamma}}{(P_{\text{prv}})^{2/\gamma}} - \frac{(P_{\text{cfav}})^{(1-\gamma)/\gamma}}{(P_{\text{prv}})^{(\gamma+1)/\gamma}}}{\left(\frac{\gamma-1}{2}\right)\left(\frac{2}{\gamma+1}\right)^{\frac{\gamma+1}{\gamma-1}}}\right]^{1/2}. \tag{17}$$

The parameter γ is the specific heat ratio of the air Van Wylen et al. (1998).

In the light of the model presented in equations from 1 to 5, the control current i modulates the FAV's torque motor areas and, thus, allows the FAV opening chamber to be pressurized (or depressurized) according to dynamics presented in Eq. 2. The pressure in the opening chamber of the valve forces the piston actuator against the spring, modifying the opening angle of the valve's butterfly (the dynamics of the valve's actuator is according to Eq. 3). By modifying the butterfly's opening angle, it also modifies the effective area of the valve, modulating the amount of cold air flowing through the valve and pressurizing the duct volume in the inlet of the heat exchanger (as per dynamics given in Eq. 1). Then, the cold air flows through the heat exchanger, and the hot air is cooled down, with temperature dynamics governed by Eq. 4. Finally, the temperature of the cooled air downstream the heat exchanger is measured by a temperature sensor, and its dynamics is given according to Eq. 5.

As previously mentioned, the entire system is nonlinear. However, as per the control approach proposed in this work, only the nonlinearities from dynamics of Eqs. 2 and 3 are explored, given the differential flatness property of the FAV. Regarding the nonlinear dynamics of P_{cin}, the input variable is the FAV piston position x_v (as per Eq. 1), and in a steady-state condition, one has x_v constant. Considering small variations around an equilibrium point, both f_0 and f_2 can be approximated to constant values. By knowing that f_0 has a negative value (refer to Eq. 6), then by analysis of the linear approximation of Eq. 1, one can check that such dynamics is stable (given stability of its input x_v). Similar analysis can be performed for the nonlinear dynamics given in Eqs. 4 and 5 , and from their linear approximations, one can verify the stability of T_{Hout2} and T_{Hout3}, respectively. Moreover, the effects related to the nonlinear dynamics of the variables T_{Hout2} and T_{Hout3} are addressed by considering reduced gains for the control loop in which such variables are relevant. Details about the control strategies evaluated in this work are presented in the next section.

5 Control Strategy

Given the system represented in the schematic of Fig. 1, the objective in this work is to explore the use of flatness technique in order to control the system output T_{Hout3}, comparing the results with those achieved by a simple PID. Specifically, the scenario in which system windup occurs is evaluated, mainly because during such condition, the temperature T_{Hout3} may reach high values during system's transient. Due to safety concerns, the highest value of T_{Hout3} should not reach 260 °C.

Four different strategies have been evaluated. In order to refer to them in a simple manner, they are nominated as follows:

1. Flatness (Flat);
2. Simple PID, without any anti-windup technique (PID);
3. PID with anti-windup technique (PID anti-windup);
4. Flatness as feedforward compensator, combined with a PID ($Flat\ \&\ PID$)—main purpose of this work.

Schematics showing the architecture of each control technique evaluated are provided in Figs. 3, 4 and 5. For the strategy $Flat$, which was previously proposed in Silva and Yoneyama (2018), the architecture control is composed of two loops: an inner loop for the position control of the FAV and an outer loop for FAV position reference generation, based on the error between desired and measured temperature at the outlet of the heat exchanger hot side. The PID and PID anti-windup techniques have a traditional architecture. Finally, as one can see in Fig. 5, the proposed $Flat\ \&\ PID$ technique is a combination between the two last mentioned architectures. With such structure, the integrator is allowed to windup until it reaches its saturation, and after an upset in the system, the regulator can act fast enough due to the contribution of the control current calculated using the flatness technique (identified, in Fig. 5, as the dynamic BIAS of the PID).

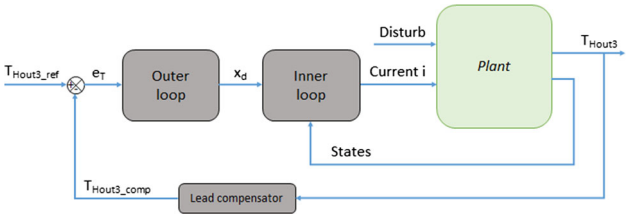

Fig. 3 Schematic of control strategy: Flat

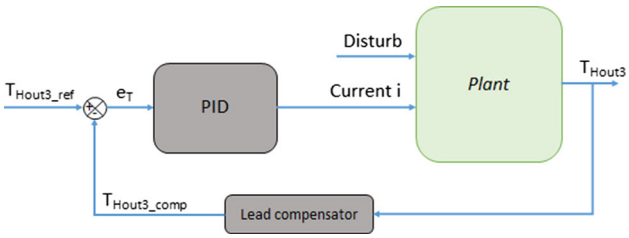

Fig. 4 Schematic of control strategies: PID and PID anti-windup

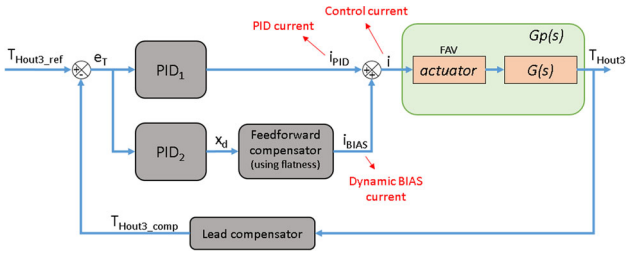

Fig. 5 Schematic of control strategy: *Flat & PID*

As per the schematic shown in Fig. 5, the control strategy being proposed comprises:

- PID_1: generates the PID control current for the actuator (FAV), based on the temperature control error;
- PID_2: generates a position reference for the actuator (FAV), also based on the temperature control error;
- *Feedforward compensator (flatness-based)*: generates the additional control current for the actuator (FAV), based on the position reference resulted from the PID_2.

5.1 Flatness (Flat)

5.1.1 Inner Loop: FAV Position Control Using Flatness

The expressions for $\dot{P}_{\text{cfav}}$ and $\ddot{x}_v$ are according to Eqs. 2 and 3, respectively. They are intentionally repeated below:

$$\dot{P}_{\text{cfav}} = f_1 P_{\text{cfav}} + f_3 i, \tag{18}$$

$$\ddot{x}_v = \frac{A_1}{m} P_{\text{cfav}} - \frac{b}{m}\dot{x}_v - \frac{K_m}{m}x_v - \frac{A_2}{m}P_{\text{amb}} - \frac{P_L}{m}. \tag{19}$$

By isolating P_{cfav} from 19,

$$P_{\text{cfav}} = \frac{m}{A_1}\left(\ddot{x}_v + \frac{b}{m}\dot{x}_v + \frac{K_m}{m}x_v + \frac{A_2}{m}P_{\text{amb}} + \frac{P_L}{m}\right), \tag{20}$$

and differentiating 20 once:

$$\dot{P}_{\text{cfav}} = \frac{m}{A_1}\left(x_v^{(3)} + \frac{b}{m}\ddot{x}_v + \frac{K_m}{m}\dot{x}_v + \frac{A_2}{m}\dot{P}_{\text{amb}}\right), \tag{21}$$

Substituting 20 and 21 in 18, one gets:

$$\begin{aligned} i = {} & \frac{1}{f_3}\left[\frac{m}{A_1}x_v^{(3)} + \left(\frac{b}{A_1} - f_1\frac{m}{A_1}\right)\ddot{x}_v\right] \\ & + \frac{1}{f_3}\left[\left(\frac{K_m}{A_1} - f_1\frac{b}{A_1}\right)\dot{x}_v - f_1\frac{K_m}{A_1}x_v\right] \\ & + \frac{1}{f_3}\left[\frac{A_2}{A_1}\dot{P}_{\text{amb}} - f_1\frac{A_2}{A_1}P_{\text{amb}} - f_1\frac{1}{A_1}P_L\right]. \end{aligned} \tag{22}$$

Considering constant mean values for f_1 and f_3, and also taking into account that the ambient pressure P_{amb} evolves slowly, one can make the approximation $\dot{P}_{\text{amb}} \approx 0$ (i.e., the dynamics of the system is much faster than the dynamics of P_{amb}, such that its *exogenous* characteristic can be, at first, disregarded). Then, P_{cfav} and i can be both expressed as functions of x_v and a finite number of its derivatives. Thus, the system formed by Eqs. 18 and 19 is flat, with x_v as the flat output.

By setting $x_v = x_d$, in which x_d is the desired value for the position x_v of the valve, the control current i given in 22 is rewritten in 23. Since there are no closed-loop actions to control the position x_v, a steady-state error is expected for this signal. Nevertheless, the temperature at the outlet of the heat exchanger hot side is kept at its reference value with no steady-state error, since the aforementioned error in the inner loop is compensated by the outer loop.

$$\begin{aligned} i = {} & \frac{1}{f_3}\left[\frac{m}{A_1}x_d^{(3)} + \left(\frac{b}{A_1} - f_1\frac{m}{A_1}\right)\ddot{x}_d\right] \\ & + \frac{1}{f_3}\left[\left(\frac{K_m}{A_1} - f_1\frac{b}{A_1}\right)\dot{x}_d - f_1\frac{K_m}{A_1}x_d\right] \\ & + \frac{1}{f_3}\left[\frac{A_2}{A_1}\dot{P}_{\text{amb}} - f_1\frac{A_2}{A_1}P_{\text{amb}} - f_1\frac{1}{A_1}P_L\right]. \end{aligned} \tag{23}$$

5.1.2 Outer Loop: FAV Position Reference Generation Using a PID

The outer loop is the one responsible for closing the temperature control loop and consists of a lead compensator in cascade with a PID controller. This loop generates the reference value for the FAV piston position, x_d, required by the inner loop. The equations are presented from 24 to 26.

$$T_{\text{Hout3\_comp}} = T_{\text{Hout3}} \frac{T_{lc}s + 1}{\alpha_{lc} T_{lc}s + 1}, \tag{24}$$

where $T_{\text{Hout3\_comp}}$ is the compensated measured temperature, and s is the argument of the Laplace transform. Also, T_{lc} and α_{lc} are the parameters from the lead compensator.

The objective of the lead compensator is to "recover" the phase margin that is "lost" due to the inherent thermal inertia (heat exchanger and temperature sensor, usually a RTD type). Using simulation for its design, the parameter T_{lc} was adjusted to the same value of parameter τ_s and, for the parameter α_{lc}, which shall not be too small in order to avoid high noise amplification, the value adopted was 0.1.

Denoting by $T_{\text{Hout3\_ref}}$ the desired value of the temperature $T_{\text{Hout3\_comp}}$, the reference value for the control variable x_v is given by 25.

$$x_d = -k_{p\_\text{outer}} e_T - k_{i\_\text{outer}} \int e_T - k_{d\_\text{outer}} \frac{\mathrm{d}e_T}{\mathrm{d}t}, \tag{25}$$

in which e_T is the temperature error, given by 26:

$$e_T = T_{\text{Hout3\_ref}} - T_{\text{Hout3\_comp}}. \tag{26}$$

Since the lead compensator has unitary gain, one has in steady-state that $T_{\text{Hout3\_comp}} \rightarrow T_{\text{Hout3}}$. The proportional, integral and derivative gains (k_{p_outer}, k_{i_outer} and k_{d_outer}) were adjusted in such a way that the outer loop was slower than the inner loop, so that coupling between the control loops is avoided.

5.2 Simple PID (PID)

The second technique, which is also presented in Silva and Yoneyama (2018), is a lead compensator in series with a simple PID. The equations are the same as presented for the outer loop of Sect. 5.1.2. The purpose of such technique evaluation was to create a comparison standard for all the other techniques, since it is the traditional control technique applied to the control of aeronautical pneumatic systems.

The control current i, obtained for the simple PID control technique, is presented in Eq. 27.

$$i = -k_{p\_\text{pid}} e_T - k_{i\_\text{pid}} \int_0^t e_T \mathrm{d}t - k_{d\_\text{pid}} \frac{\mathrm{d}e_T}{\mathrm{d}t}. \tag{27}$$

The gains proportional, integral and derivative were adjusted by trial and error, such that system could be properly controlled without temperature oscillation.

5.3 PID with Anti-windup (PID Anti-windup)

The third technique, PID anti-windup, has basically the same structure as presented for the simple PID. However, it has additional logic aimed at avoiding the integrator from winding up. The anti-windup logic applied in this study is based on the back-calculation method described in Astrom and Rundqwist (1989). The method works as follows: When the actuator output saturates, the integral is recomputed so that its new value gives an output at the saturation limit. Consider the regulator schematic shown in Fig. 6, and the difference $e_t(t)$ between the output of the regulator $v(t)$ and the actuator output $u(t)$ is fed to the input of the integrator through a gain $1/T_t$. The signal $e_t(t)$ is zero when there is no saturation. Thus, it has no effect on the normal operation when the actuator does not saturate. When the actuator saturates, the feedback signal prevents the integrator from winding up. The time constant T_t determines how quickly the integrator of the PID controller is reset. If the actual output $u(t)$ of the actuator is not measurable, one can use a mathematical model of the actuator.

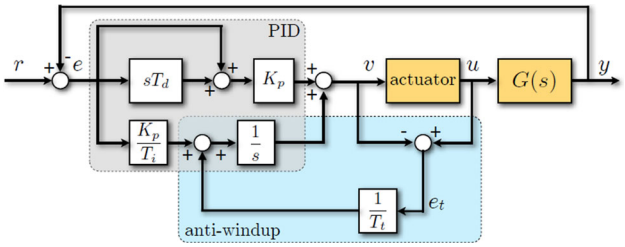

Fig. 6 Regulator with anti-windup based on back-calculation Bemporad (2010)

In order to evaluate the anti-windup methodology presented in Fig. 6, a similar method was implemented as follows: The integral part of the PID is frozen when the FAV's piston position reaches 2 % of its maximum stroke (i.e., if $x_v < 2$ or $x_v > 98$), and it is allowed to operate normally if the FAV's piston position is within the referred band. However, the FAV's position measurement is not required for the simple PID technique implementation. By considering the aforementioned anti-windup logic, such parameter becomes necessary since the actuator's position is an input for it. Other possibility is to use a model to represent the actuator's saturation (e.g., FAV's position as a function of control current i), but one must consider the model uncertainties (manufacturing variations, aging, etc.), and consequently, the effectiveness of the anti-windup logic will be degraded. In this evaluation, the FAV's position measurement was considered as available.

5.4 Flatness as Feedforward Compensator, Combined with a PID (*Flat & PID*)

The fourth and main technique presented in this study is the use of flatness-based control combine with a PID. In essence, it is a junction of the techniques flatness (described

in Sect. 5.1) and simple PID (described in Sect. 5.2). With such structure, the integrator of the PID is allowed to wind up until it reaches its saturation, and after an upset in the system, the regulator can act fast enough due to the contribution of the control current calculated using the flatness technique.

One can observe, in the schematic of Fig. 5, that the control current i is the combination of the current calculated by the simple PID technique (i_{PID} from block PID_1) and the current calculated by the flatness technique (here defined as i_{BIAS}). The block PID_2 refers to outer loop described in Sect. 5.1.2. Thus, the expression for the control current i is equivalent to the sum of expressions presented in Eqs. 23 and 27, and it is given in Eq. 28.

$$
\begin{aligned}
i = & \left(-k_{p\_\text{pid}} e_T - k_{i\_\text{pid}} \int_0^t e_T \mathrm{d}t - k_{d\_\text{pid}} \frac{\mathrm{d}e_T}{\mathrm{d}t}\right) \\
& + \frac{1}{f_3}\left[\frac{m}{A_1} x_d^{(3)} + \left(\frac{b}{A_1} - f_1 \frac{m}{A_1}\right) \ddot{x}_d\right] \\
& + \frac{1}{f_3}\left[\left(\frac{K_m}{A_1} - f_1 \frac{b}{A_1}\right) \dot{x}_d - f_1 \frac{K_m}{A_1} x_d\right] \\
& + \frac{1}{f_3}\left[\frac{A_2}{A_1} \dot{P}_{\text{amb}} - f_1 \frac{A_2}{A_1} P_{\text{amb}} - f_1 \frac{1}{A_1} P_L\right],
\end{aligned} \tag{28}
$$

in which x_d is the desired value for the position x_v of the FAV, calculated according to Eq. 25.

Unlike the anti-windup logic presented in the previous section, the FAV's position measurement is not required for this strategy proposal. Simulation results, for both implementations, are shown in the next section.

6 Simulation Results and Discussion

When designing the control laws for pneumatic systems, an important scenario that must be evaluated is related to the condition in which the bleed inlet temperature is low enough to be below the system's temperature reference, so that the FAV operates at fully closed position. Under such condition, the control techniques that make use of integral action may be exposed to the windup phenomenon. The integral term and the controller output, as well, may become really large and, consequently, leading to undesirable overshoots in the system.

Thus, seeking to obtain the performance of the proposed control architecture (i.e., flatness as feedforward compensator, combined with a PID—strategy 4) under the referred condition and compare to the other three strategies evaluated in this study, simulation was performed considering a scenario in which the engine is accelerated, from idle to take-off thrust level, but the bleed inlet temperature is initially at 185 °C (lower than the temperature reference of 200 °C).

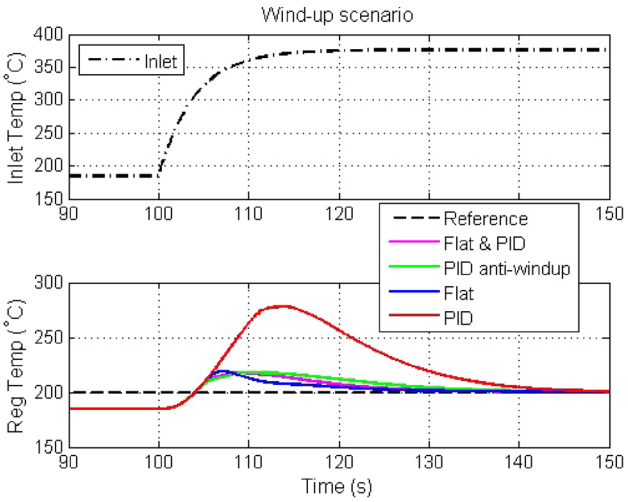

Fig. 7 Regulated temperature T_{Hout3}, during engine acceleration and windup scenario

Once the engine is accelerated, the bleed inlet temperature is increased up to 370 °C.

First, in Fig. 7, it is shown the regulated temperature T_{Hout3} for the windup scenario. During the transient, the maximum temperature reached when using the combination flatness (Flat) and simple PID, identified in the figure as $Flat \,\&\, PID$, was approximately 218 °C, which was quite similar to results of 213 °C of the flatness (Flat) technique. Comparatively, when using the PID technique with the anti-windup logic, the temperature reached 219 °C, which is much lower than the result of 278 °C obtained with the simple PID without the anti-windup logic.

The FAV's piston position and the control current i, for the windup scenario, are shown in Fig. 8 and in Fig. 9, respectively. From such figures, it is possible to see that the feedforward compensation provided by the flatness technique when combined to the PID does allow the control to fast react during system upset in a windup scenario.

The behavior of the control current i obtained with the $Flat \,\&\, PID$, shown in Fig. 9, is the combination of the current obtained with the PID technique and the current obtained with the flatness (Flat).

Additionally, a full flight profile simulation was also performed. Figure 10 shows the phases experienced by an aircraft during the flight. The phases are: A—takeoff, B—climb, C—cruise, D—descent, E—holding, and F—landing. At the beginning, the system was operating only supplying air for cabin pressurization and air conditioning. When aircraft crosses 10 kft, the anti-ice system is activated and the pneumatic system temperature reference is increased from 200 to 230 °C, since there is a higher energy demand in the system in order to heat up the aircraft wing's leading edge and avoid ice formation. At 15 kft, the anti-ice system is

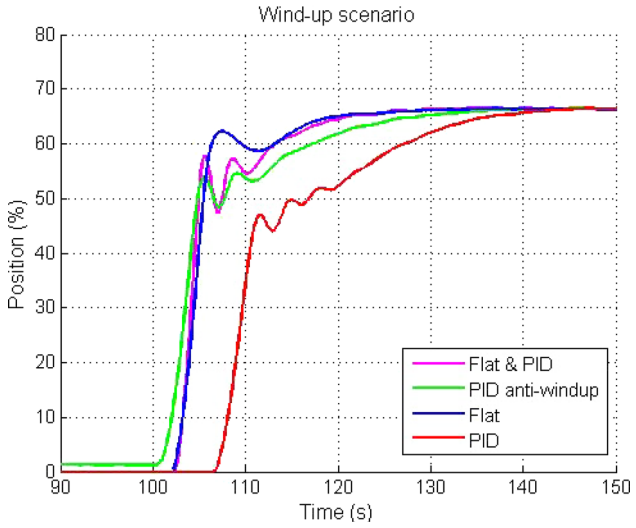

Fig. 8 FAV's piston position x_v, during engine acceleration and windup scenario

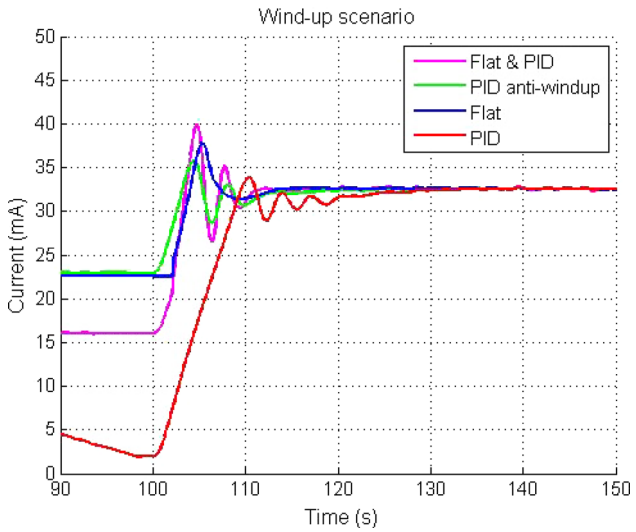

Fig. 9 Control current i, during engine acceleration and windup scenario

deactivated and kept off during the remaining flight, and also the temperature reference is set back to 200 °C.

Unlike the previous scenario, for the full flight simulation, there is no windup condition. The results are presented in Figs. 11, 12 and 13, showing the regulated temperature T_{Hout3}, the FAV's piston position x_v and the control current i, respectively.

As one can observe, the system could be properly controlled considering the four strategies evaluated herein, specially with the approach in which flatness is combined with a PID ($Flat\ \&\ PID$). In Fig. 13, it is possible to verify that when such control strategy is applied (i.e., $Flat\ \&\ PID$), the control current presents larger amplitude in the transient, mainly during anti-ice activation and deactivation, but with-

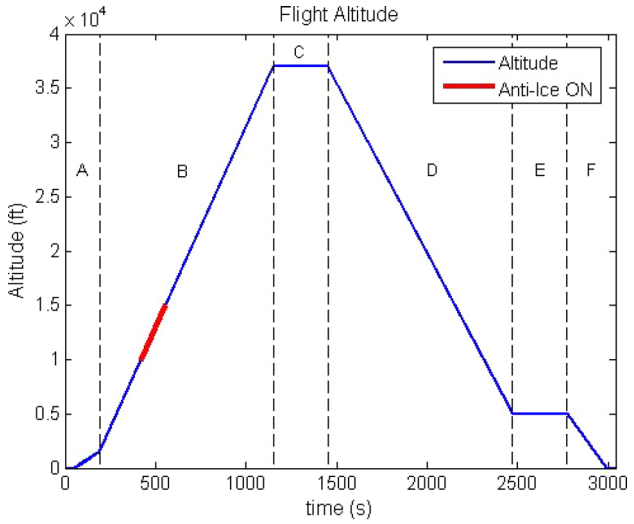

Fig. 10 Aircraft's flight profile

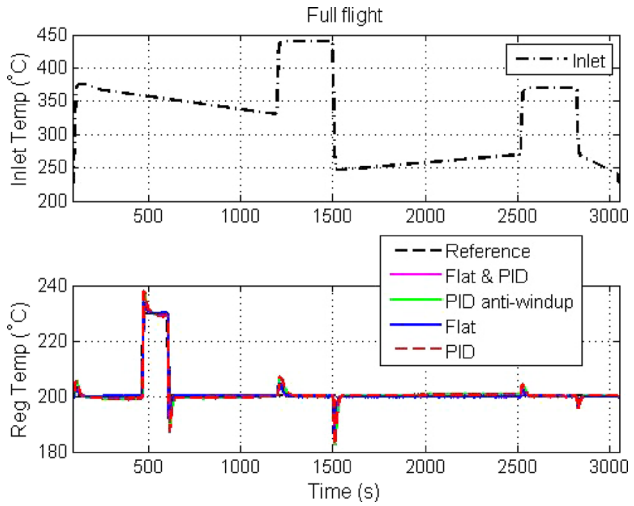

Fig. 11 Regulated temperature T_{Hout3}, during full flight

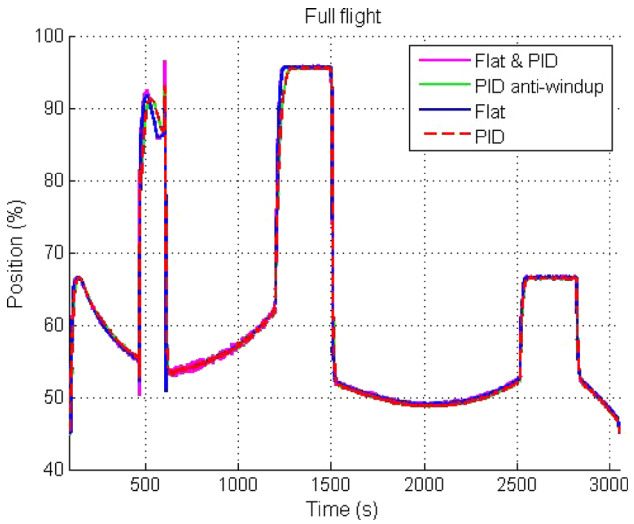

Fig. 12 FAV's piston position x_v, during full flight

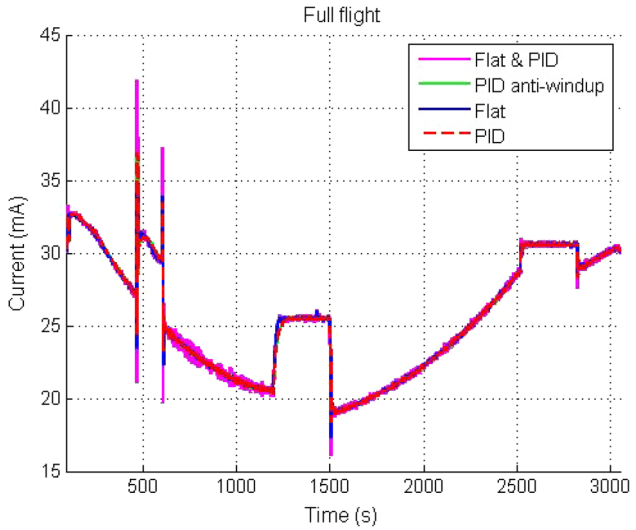

Fig. 13 Control current i, during full flight

out leading the actuator to saturate and, thus, providing good performance to the system.

7 Conclusion

The controller design method based on flatness theory combined with a PID was assessed in the context of temperature control of an aeronautical pneumatic system. More specifically, the proposed control strategy was evaluated for the condition in which the system is exposed to the windup scenario. For comparison purpose, other strategies [e.g., PID and flatness architecture as proposed in Silva and Yoneyama (2018)] were also evaluated.

The combination of flatness and PID ($Flat\ \&\ PID$), with the flatness acting like a feedforward compensator, has shown to be a good alternative to counteract the effects during an upset after the integrator has wound-up, without the necessity of measuring the position of the actuator (in this case the FAV). Better than this, it allows the system to achieve the good performance enabled by the Flat technique and, in parallel, keeps the use of the traditional PID that is highly acknowledged in the aeronautical industry.

References

Andersen, B. W. (2001). *The analysis and design of pneumatic systems* (3rd ed.). Florida: Krieger Publishing Company.

Astrom, K. J., & Rundqwist, L. (1989). Integrator windup and how to avoid it. In *Proceedings of American Control Conference* (pp. 1693–1698). Pittsburgh, PA, USA: IEEE.

Bemporad, A. (2010). *Anti-windup techniques*. Trento, TN: University of Trento. http://cse.lab.imtlucca.it/~bemporad/teaching/ac/pdf/AC2-09-AntiWindup.pdf. Accessed on November 5, 2018.

Fliess, M., Levine, J., Martin, P., & Rouchon, P. (1995). Flatness and defect of non-linear systems: Introductory theory and examples. *International Journal of Control*, *61*(6), 1327–1361.

Fliess, M., Levine, J., Martin, P., & Rouchon, P. (1999). A lie-backlund approach to equivalence and flatness of nonlinear systems. *IEEE Transactions on Automatic Control*, *44*(5), 922–937.

Hadade Neto, A. (2005). *Tecnicas anti-windup em estruturas de controle pid, rst e gpc*. Mestrado em engenharia: Universidade Federal de Santa Catarina, Florianópolis.

Incropera, F. P., & Dewitt, D. P. (1998). *Fundamental of heat and mass transfer* (4th ed.). Rio de Janeiro: LTC.

Koo, T. J., Ma, Y., & Sastry, S. S. (2001) . Nonlinear control of a helicopter based unmanned aerial vehicle model. Technical report, UC Berkeley

Koo, T. J., Sastry, S. (1999). Differential flatness based full authority helicopter control design. In *Proceedings of Conference on Decision and Control*. Phoenix, Arizona USA

Martin, P. (1994). A different look at output tracking: Control of a VTOL aircraft. In *Proceedings of Conference on Decision and Control*. Lake Buena Vista, Florida USA

Martin, P. (1996) . Aircraft control using flatness. In *Proceedings of CESA'96 IMACS Multiconference—Symposium on Control, Optimization and Supervision*. Lille, France

Ogata, K. (2003). *Modern control engineering* (4th ed.). Sao Paulo: Prentice Hall.

Rigatos, G., Siano, P., & Arsie, I. (2016). A differential flatness theory approach to embedded adaptive control of turbocharged diesel engines. *Intelligent Industrial Systems*, *2*(4), 349–370.

Silva, D. D., Tannuri, E. A., & Turcio, W. (2014). Temperature control of an aeronautical pneumatic system using feedback linearization and pid. In *Proceedings of Mediterranean Conference on Control and Automation*. Palermo, Italy

Silva, D. D., & Yoneyama, T. (2018). Nonlinear control of an aeronautical pneumatic system. *Journal of Control, Automation and Electrical Systems*, *29*(3), 292–302.

Turcio, W., Yoneyama, T., & Moreira, F. (2013). Quasi-LPV gain-scheduling control of a nonlinear aircraft pneumatic system. In *Proceedings of Mediterranean Conference on Control and Automation*. Planatanias-Chania

Turcio, W, Yoneyama, T, & Silva, D. D. (2014). Control of an aeronautical pneumatic system using feedback linearization. In *Proceedings of Mediterranean Conference on Control and Automation*. Palermo, Italy

Van Wylen, G., Sonntag, R. E., & Borgnakke, C. (1998). *Fundamental of thermodynamics* (5th ed.). Sao Paulo: Edgard Blucher.